ARTICLE

Oxidation of Carbon Supports at Fuel Cell Cathodes: Differential Electrochemical Mass Spectrometric Study

Ming-fang Li[a], Qian Tao[a], Ling-wen Liao[a], Jie Xu[a], Jun Cai[b], Yan-xia Chen[a*]

a. Hefei National Laboratory for Physical Sciences at Microscale, Department of Chemical Physics, University of Science and Technology of China, Hefei 230026, China
b. Department of Optics and Optical Engineering, University of Science and Technology of China, Hefei 230026, China

(Dated: Received on January 11, 2010; Accepted on June 4, 2010)

The effects of O_2 and the supported Pt nano-particles on the mechanisms and kinetics of the carbon support corrosion are investigated by monitoring the CO_2 production using differential electrochemical mass spectrometry in a dual-thin layer flow cell. Carbon can be oxidized in different distinct potential regimes; O_2 accelerates carbon oxidation, the rates of CO_2 production from carbon oxidation in O_2 saturated solution are two times of that in N_2 saturated solution at the same potential; Pt can catalyze the carbon oxidation, with supported Pt nanoparticles, the overpotential for carbon oxidation is much smaller than that without loading in the carbon electrode. The mechanism for the enhanced carbon oxidation by Pt and O_2 are discussed.

Key words: Carbon corrosion, Pt, Fuel cell cathode, Differential electrochemical mass spectrometry

I. INTRODUCTION

Nano-structured carbon materials, such as carbon black, carbon fiber, carbon nanotubes, and so on, are widely used as the support for the noble metal electrocatalysts in polymer electrolyte membrane fuel cells (PEMFCs), due to their high electrical conductivity, chemical stability, and low cost [1−4]. Carbon supports can help to reduce the noble metal loadings by stabilizing the small metal nano-particles supported on it and help to improve the conductivity and the mass transport of reactants and products in the electrodes of PEMFCs [1, 2]. However, under the conditions where PEMFC cathode operates, *i.e.*, in environment with high oxygen concentration, high potential (0.6−1.2 V) and high temperature (50−90 °C) as well as high acidity and humidity, electrochemical oxidation of the carbon supports takes place [5−7]. As carbon is oxidized, the nano-catalysts aggregate into larger particles or even fall off from the support, which results in a decrease in the active surface area of the nano-catalysts, consequently lead to a reduced performance and operation lifetime of the PEMFCs [3, 6, 8−10]. In order to avoid carbon oxidation, fundamental studies on the mechanism of carbon oxidation as well as factors which affect the kinetics of carbon oxidation are necessary.

A number of studies reveal that the carbon support can be reversibly oxidized to oxygenated functionals such as carboxylic, phenolic, lactonic, and etheric groups [5, 11, 12]; in the PEMFCs, irreversible oxidation of the carbon supports to CO_2 is also confirmed [10, 13, 14]. It is confirmed that the supported Pt nanoparticles accelerate the corrosion of carbon black under PEMFCs conditions [4, 5, 7, 10] are similar to the case in phosphoric acid fuel cell (PAFC) [15, 16]. However, by now it is not clear how Pt promotes the carbon oxidation.

In order to better understand the mechanism and kinetics of carbon oxidation, we investigated the carbon oxidation in a dual-thin layer flow cell with saturated N_2 and O_2 solution respectively. The flow cell allows to simultaneous mass spectrometric and electrochemical measurements under controlled mass transport conditions [17], in contrast to earlier approaches investigated in real PEMFCs, measurements conducted under such conditions can be much better defined and carbon oxidation mechanisms are better understood. The roles of O_2 and supported Pt nanoparticles in the kinetics and mechanism of carbon oxidation were examined by monitoring the evolution CO_2 at the working electrode consisted of carbon support with or without Pt nanoparticles and in the cases in the existence and absence of O_2.

*Author to whom correspondence should be addressed. E-mail: yachen@ustc.edu.cn

II. EXPERIMENTS

The dual-thin layer flow cell used for the present differential electrochemical mass spectrometry (DEMS) study is the same as that reported by Chen *et al.* [18], except that the 2nd compartment is mounted with a porous polytetrafluoroethylene (PTFE) membrane (60 μm thick, 50% porosity and 0.2 μm pore diameter, Scimat) which forms one of the walls and simultaneously the interface to the vacuum system. The electrolyte flow was enforced by the hydrostatic pressure in the supply bottle (electrolyte flow rate is about 30 μL/s), ensuring a fast transport of the species formed at the electrode to the mass spectrometric compartment, where the volatile products were evaporated into the MS through a porous PTFE membrane, allowing simultaneous measurements of the Faradic current at the working electrode and the mass signals of volatile products (side products) produced during the reaction. Two Pt foils were used as the counter electrodes. A reversible hydrogen electrode (RHE) was served as a reference electrode. The electrode potential was controlled by PAR 273A potentiostat (Princeton Applied Research). All potentials are quoted against the RHE. All experiments were carried out at ambient temperature ((25±1) °C).

Before each experiment the glassy carbon electrodes (GC, 6 mm in diameter, Tianjin Aida Hengsheng Tech Co. China) were polished to a mirror finishing with 0.1 μm alumina suspension, followed by ultrasonicating in acetone and Millipore Q water each for 10 min, and the process was repeated three times. The reactant ink was prepared by ultrasonically dispersing either 8.0 mg carbon black (Vulcan XC 72) or 10 mg Pt/Vulcan XC-72 (20% Pt, E-TEK Inc.) mixed with 10 μL 10% nafion solution (Dupont co.) in 10 mL isopropanol for about 20 min. The thin-film working electrodes for the DEMS measurements were prepared by pipetting 15 μL of this suspension (carbon material 0.8 g/L) onto the GC disks, which were then dried under continuous N_2 stream. The loadings of carbon black and Pt nanoparticles in terms of the working area of the GC electrode (diameter of 5 mm; area of 0.196 cm^2) are 61.2 and 15.3 $\mu g/cm^2$, respectively.

0.5 mol/L H_2SO_4 was used as supporting electrolyte and was prepared using Millipore Q water and ultrapure sulfuric acid (Sinophram Chemical Reagent Co., Ltd., China). During the measurements, the electrolyte was either saturated with N_2 or O_2 (Nanjing Special Gas Corp., 5N) through continuously purging of the electrolyte with respective gas. Before DEMS measurement, the cleanness of all electrodes was checked by cyclic voltammetry in the DEMS cell in the potential region from 0.05 V to 1.3 V at a scan rate of 100 mV/s in N_2 saturated 0.5 mol/L H_2SO_4 solution. Carbon corrosion was examined by cyclic voltammerty in the potential region from 0.05 V to 1.2 V at a sweep rate of 10 mV/s, and mass spectrometric signal of CO_2 (m/z=44) was simultaneously recorded using a quadrupole mass spectrometer (Hiden, HPR-40).

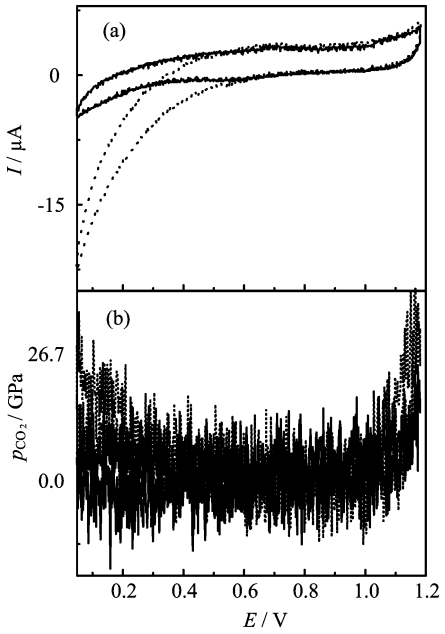

FIG. 1 (a) Cyclic voltammorgam (CV) and (b) mass spectrometric cyclic voltammorgram (MSCVs) of Vulcan XC72 nano-particle electrodes in oxygen saturated (solid line) and nitrogen saturated (dotted line) 0.5 mol/L H_2SO_4 solution, scan rate 10 mV/s.

III. RESULTS AND DISCUSSION

Figure 1 (a) and (b) shows the cyclic voltammorgams (CVs) and mass spectrometric cyclic voltamorgrams (MSCVs) of the carbon electrode made of powders of Vulcan XC-72 in N_2 and O_2 saturated 0.5 mol/L H_2SO_4, respectively. The base CV of the carbon electrode in N_2 saturated solution displays two small peaks at 0.7 V in the positive-going and at 0.6 V in the negative-going scan, respectively. Since no CO_2 signals are detected by DEMS at these potentials, the peaks are assigned to the reversible formation/reduction of surface oxides at the carbon support [19, 20]. In O_2 saturated solution, the I-E curves at E>0.6 V are nearly the same as that in N_2 saturated solution, while at E<0.35 V, cathodic current from oxygen reduction reaction at carbon electrode increases with decreasing in electrode potential.

From the simultaneously recorded MSCVs of CO_2 production from carbon electrodes (Fig.1(b)), mass signals of CO_2 are observed in two distinct potential region in both positive- and negative-going potential scan: (i) at E<0.3 V, there is an increase in the rates of CO_2 production with decreasing in electrode potential; (ii) at E>1.1 V, CO_2 signal increases monotonically with elec-

DOI:10.1088/1674-0068/23/04/442-446

trode toward positive potentials. The CO_2 produced at E<0.3 V is close to or even below the standard potential of electrochemical oxidation carbon according to the following reaction:

$$C + 2H_2O \rightarrow CO_2 + 4H^+ + 4e^- \quad (1)$$
$$E^{\ominus} = 0.207\ V_{RHE}$$

The increase in CO_2 production rate with decreasing electrode potential suggests that produced CO_2 may not originate from the direct electrochemical oxidation of carbon to CO_2. Referring to the facts that (i) at E<0.3 V, only cathodic current is observed (Fig.1) and (ii) on pure carbon electrode, dominant product formed from oxygen reduction at potentials negative of 0.3 V is H_2O_2 and whose production rate increases with decreasing in electrode potential [21], it is concluded that CO_2 produced at E<0.3 V is from the catalytic oxidation of carbon by H_2O_2 produced from O_2 reduction.

The second wave for CO_2 production appears at E>1.1 V in N_2 saturated solution, while in O_2 saturated solution, the ignition potential shift negatively to 1.0 V. Furthermore, from Fig.1 it can be clearly seen that the trends of carbon oxidation are the same in both N_2 and O_2 saturated solution, except that CO_2 signal in O_2 saturated solution is almost double of that in N_2 saturated solution at the same potential. Furthermore, it is noticed that, toward positive potentials there is a simultaneous increase in anodic Faradaic current with CO_2 mass signal, which suggests that CO_2 is produced through electrochemical oxidation of carbon electrode. Though oxygen functional groups can be formed on carbon electrode at potential as low as 0.207 V according to the reaction Eq.(1), high overpotential is necessary in order to oxidize these intermediates. The enhanced carbon oxidation in O_2 saturated solution suggests that O_2 is directly involved in the carbon oxidation, while in N_2 saturated solution, carbon is mostly oxidized through the decomposition of water from the electrolyte. In addition, it is noticed that in the negative-going scan, the rate of CO_2 production is nearly the same as that in the positive-going scan at the same potential.

Figure 2 (a) and (b) shows the CVs and MSCVs of the electrode of Pt nanoparticles supported on Vulcan XC-72 in N_2 and O_2 saturated 0.5 mol/L H_2SO_4, respectively. The base CV of the carbon supported Pt nanoparticle electrode in N_2 saturated solution displays typical current peaks for the adsorption/desorption H atoms in the potential region from 0.05 V to 0.35 V, the anodic current of Pt oxidation starts to increase at ca. 0.80 V and achieves a local maximum at 1.0 V, which is followed with a reduction peak at 0.75 V in the negative-going scan. In O_2 saturated solution, oxygen reduction reaction (ORR) current flow at E<0.9 V increases with the decreasing in electrode potential with a half wave potential of 0.80 V, at E<0.6 V the mass diffusion limited current is reached and at E<0.4 V, currents from H_{upd} (under potential deposition of H)

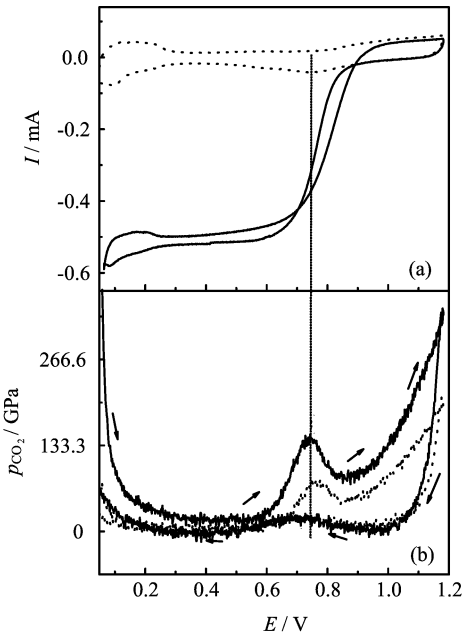

FIG. 2 CV (a) and MSCVs (b) of Vulcan XC72 supported Pt nano-particle electrodes in oxygen saturated (solid line) and nitrogen saturated (dotted line) 0.5 mol/L H_2SO_4 solution, scan rate 10 mV/s.

are superimposed on the ORR currents. From Fig.2 it is also seen that at E>0.7 V, the ORR activity in the negative-going scan is lower (with an overpotential of ca. 30 mV to 50 mV higher) than that in the positive-going scan. This effect can be explained by the poisoning of Pt surface by oxide and OH species which initially formed at higher potentials in the positive-going scan [22].

From the MSCVs of CO_2 signal measured at carbon supported Pt nanoparitcle electrodes (Fig.2(b)), it is clearly seen that in both positive- and negative-going potential scan there are three potential regions where CO_2 is produced: (i) in the potential region from 0.05 V to 0.3 V, there is an increase in the mass signal of CO_2 with the decreasing in electrode potential as similar to the case of pure carbon electrode; (ii) in the potential region from 0.6 V to 0.9 V, there is a peak for CO_2 production with peak potential of 0.75 V; (iii) at E>0.9 V, CO_2 signal increases monotonically with electrode toward positive potentials. In addition, it is noticed that in the negative-going scan, the CO_2 production rates in the three potential regions mentioned above are much smaller than that in the corresponding positive-going scan, which is in contrast to the case of pure carbon electrode (Fig.1). Furthermore, it is found that the trends of carbon oxidation at Pt/C electrode in O_2 saturated solution are also the same as that in N_2 saturated solution, while CO_2 signal in O_2 saturated solution is nearly two times of that that in N_2 saturated solution at the same potential. Since the trends of CO_2 production

DOI:10.1088/1674-0068/23/04/442-446

from carbon oxidation in O_2 saturated solution are the same as that in N_2 saturated solution on both types electrode, O_2 can only accelerate the carbon oxidation but not change the mechanism on both types electrode.

The CO_2 production at E<0.3 V is also attributed to carbon oxidation catalyzed by H_2O_2 produced from the incomplete O_2 reduction as that on carbon support. The production of H_2O_2 during ORR at Pt/C electrode in the H_{upd} potential region is well confirmed by RRDE measurements, but the current efficiency for H_2O_2 production due to the incomplete O_2 reduction is only 5%−6% in the H_{upd} region at 0.1 V [23]. Considering that the CO_2 signal at electrode with Pt nanoparticles is much larger than the case at pure carbon electrode in this potential region, it is concluded that synergetic promotion of carbon oxidation by both Pt and H_2O_2 operates. But it should be noticed that in such processes Pt nano-particles act as catalysts, while H_2O_2 molecules act as reactants.

Since no CO_2 is formed at pure carbon electrode in the potential region from 0.6 V to 0.9 V (Fig.1), CO_2 produced in this potential region must be correlated with the supported Pt nanoparticles. The peak position of the CO_2 mass signal produced from the Pt/C electrode appears at ca. 0.75 V, which is quite close to that for the oxidation of adsorbed CO at Pt. From a similar DEMS study, Willsau *et al.* found that the mass signal of CO_2 produced in the potential region from 0.6 V to 0.8 V increases after holding the potential at 0.3 and 0.45 V for 7 min, while it decreases when holding the electrode potential at 0.6 V [10]. This reveals that CO_2 produced in the potential region from 0.6 V to 0.8 V comes from the oxidation of the species formed at potentials below 0.6 V, which is most probably CO_{ad} adsorbed at Pt nanoparticles, at 0.6 V the oxidation reaction has already started, thus the amount of species at Pt surface decreases. Compared to the case in nitrogen saturated solution (Fig.2), in oxygen saturated solution the potential of this peak is ca. 20 mV negatively shifted, and the mass signal of CO_2 is almost doubled, revealing that O_2 enhances the process of CO oxidation to CO_2 on Pt.

The third CO_2 production wave at E>0.9 V is attributed to electrochemical oxidation of carbon. Compared to the case of pure carbon electrode (Fig.1), it is found that at Pt/C electrode the CO_2 production rate is greatly enhanced. Furthermore, the onset potential is negatively shifted for about 0.2 V. All these facts indicate that supported Pt nanoparticles greatly enhance the complete oxidation of carbon to CO_2. Referring to the base CV of supported Pt nanoparticles in N_2 saturated 0.5 mol/L H_2SO_4 (Fig.2), it is noticed that the anodic current of Pt oxidation starts to increase at 0.8 V and achieves a local maximum at 1.0 V. This is just opposite to the abrupt decrease in the cathodic ORR current. Since at E<1.1 V, Pt nanoparticles are only partly covered with a thin layer of OH and O_x species at their surfaces [4, 24], thus direct catalysis of C−C bond scission and C oxidation by metallic Pt is still possible. The enhanced rate for CO_2 production in O_2 saturated solution compared to that in N_2 saturated solution, suggests that PtO_x can be more easily formed from the splitting of O−O than that from H_2O decomposition. At E>1.1 V when Pt nanoparticle surface is fully covered with Pt oxides, the increase in the rate for CO_2 formation from carbon oxidation becomes slower than exponential increase as predicted by the Bultler-Volmer equation, suggesting the further covering the Pt surface with oxide will hinder the catalytic effect of Pt toward carbon oxidation. The abrupt drop in the CO_2 production rate in the negative-going scan from 1.2 V to 1.1 V further supports this.

In the negative-going scan, a small peak of CO_2 production at 0.75 V on Pt/C electrode is also discerned, which should also be related to the supported Pt nanoparticles since it was not found from carbon support electrode. Comparing to the base CV of the Pt nanoparticle electrode, it is found that the CO_2 production peak in the potential region from 0.9 V to 0.6 V mirrors well the current peak for Pt oxides reduction (Fig.2). Probably, the OH released from the reduction of Pt oxides film is involved in the carbon oxidation. In O_2 saturated solution, the mass signal for CO_2 production is the same as that in N_2 saturated solution, which further confirms that OH releases from the reduction of Pt oxides film rather than that O_2 is the reactant for the carbon oxidation.

IV. CONCLUSION

DEMS has been exploited to study the CO_2 production from the oxidation of the carbon in pure carbon electrode or in carbon support Pt nanoparticles electrode. The effects of supported Pt nanoparticles and the existence of O_2 reactants on the kinetics and mechanism of carbon oxidation have been examined.

Our results reveal that oxygen can accelerate carbon corrosion, at the same potential the CO_2 signals are nearly two times in O_2 saturated solution of that in N_2 saturated solution on both types of electrodes. Especially, in O_2 saturated solution the rate of chemical oxidation of carbon to CO_2 by H_2O_2 formed from incomplete reduction of O_2 at carbon support and Pt/C electrodes at the potential below 0.3 V, is about ten times higher than that in nitrogen saturated solution.

Supported Pt nanoparticles are found to greatly enhance the rates of the oxidation of carbon support and the subsequent CO_2 production. At Pt/C electrode, the ignition potential for the electrochemical oxidation of carbon support is 0.9 V, which is negatively shifted for more than 0.2 V. The chemical oxidation carbon by H_2O_2 produced by incomplete O_2 reduction at Pt/C electrode at E<0.3 V is also much larger than that on pure carbon electrode. Furthermore, two more CO_2 production waves from carbon oxidation are identified

DOI:10.1088/1674-0068/23/04/442-446

at Pt/C electrode than that at pure carbon electrode. One peak for CO_2 production with peak potential of 0.75 V in the positive-going scan is attributed to electrochemical oxidation of Pt-CO_{ad} or CO_{ad}-like species catalyzed by metallic Pt, while another peak of CO_2 production at 0.74 V in the negative-going scan is due to carbon oxidation by OH surface groups released from the reduction of the Pt oxides film. These results reveal that developing carbon support more stable than Vulcan XC-72 or other electronic conductive support is highly desirable in order to make PEMFCs commercially viable.

V. ACKNOWLEDGMENTS

This work was supported by the National Natural Science Foundation of China (No.20773116), the one hundred Talents' Program of the Chinese Academy of Sciences, and the National Basic Research Program of China (No.2010CB923302).

[1] C. Wang, M. Waje, X. Wang, J. M. Tang, R. C. Haddon, and Y. S. Yan, Nano Lett. **4**, 345 (2004).
[2] X. Wang, M. Waje, and Y. S. Yan, Electrochem. Solid St. Lett. **8**, A42 (2005).
[3] A. L. Dicks, J. Power Sources **156**, 128 (2006).
[4] W. Li and A. M. Lane, Electrochem. Commun. **11**, 1187 (2009).
[5] K. H. Kangasniemi, D. A. Condit, and T. D. Jarvi, J. Electrochem. Soc. **151**, E125 (2004).
[6] J. P. Meyers and R. M. Darling, J Electrochem. Soc. **153**, A1432 (2006).
[7] S. Maass, F. Finsterwalder, G. Frank, R. Hartmann, and C. Merten, J. Power Sources **176**, 444 (2008).
[8] A. A. Franco, S. Passot, P. Fugier, C. Anglade, E. Billy, L. Guetaz, N. Guillet, E. De Vito, and S. Mailley, J. Electrochem. Soc. **156**, B410 (2009).
[9] W. Schmittinger and A. Vahidi, J. Power Sources **180**, 1 (2008).
[10] J. Wilisau and J. Heitbaum, J. Electroanal. Chem. **161**, 93 (1984).
[11] J. Li, C. W. Moore, D. Bhusari, S. Prakash, and P. A. Kohl, J. Electrochem. Soc. **153**, A343 (2006).
[12] R. V. Hull, L. Li, Y. C. Xing, and C. C. Chusuei, Chem. Mater. **18**, 1780 (2006).
[13] L. C. Colmenares, A. Wurth, Z. Jusys, and R. J. Behm, J. Power Sources **190**, 14 (2009).
[14] L. M. Roen, C. H. Paik, and T. D. Jarvic, Electrochem. Solid St. Lett. **7**, A19 (2004).
[15] E. Passalacqua, P. L. Aonucci, M. Vivaldi, A. Patti, V. Antonucci, N. Giordano, and K. Kinoshita, Electrochim. Acta **37**, 2725 (1992).
[16] S. I. Pyun, Y. G. Ryu, and S. H. Choi, Carbon **32**, 161 (1994).
[17] H. Baltruschat, J. Am. Soc. Mass Spectrom. **15**, 1693 (2004).
[18] Y. X. Chen, M. Heinen, Z. Jusys, and R. B. Behm, Angew Chem. Int. Edit. **45**, 981 (2006).
[19] M. R. Tarasevich, V. A. Bogdanovskaya, and N. M. Zagudaeva, J. Electroanal. Chem. 223, (1987).
[20] H. Wolf and R. Landsberg, J. Electroanal. Chem. **29**, (1971).
[21] E. Yeager, Electrochim. Acta **29**, 1527 (1984).
[22] S. Gottesfeld, I. D. Raistrick, and S. Srinivasan, J. Electrochem. Soc. **134**, 1455 (1987).
[23] U. A. Paulus, T. J. Schmidt, H. A. Gasteiger, and R. J. Behm, J. Electroanal. Chem. **495**, 134 (2001).
[24] H. Angerstein-Kozlowska, B. E. Conway, and W. B. A. Sharp, J. Electroanal. Chem. **43**, 9 (1973).

DOI:10.1088/1674-0068/23/04/442-446